JOURNAL OF BIOMEDICAL OPTICS 3(3), 326–333 (JULY 1998)

ARTICULAR CARTILAGE OPTICAL PROPERTIES IN THE SPECTRAL RANGE 300–850 NM

Daniel W. Ebert,[†] Cynthia Roberts,[†] Stuart K. Farrar,[†] William M. Johnston,[‡] Alan S. Litsky,[*] and Alicia L. Bertone[**]

[†]The Ohio State University, Biomedical Engineering Center, 1080 Carmack Road, Columbus, Ohio 43210; [‡]The Ohio State University, College of Dentistry, Columbus, Ohio 43210; *The Ohio State University, Orthopaedic Biomaterials Laboratory, Colombus, Ohio 43210; **The Ohio State University, College of Veterinary Medicine, Columbus, Ohio 43210

(Paper JBO-129 received Jan. 10, 1997; revised manuscript received Jan. 8, 1998; accepted for publication Feb. 20, 1998.)

ABSTRACT

Measurements of absolute total reflectance were recorded from weight-bearing ($n=9$) and nonweight-bearing ($n=9$) equine articular cartilage specimens from 300 to 850 nm using a spectrophotometer with integrating sphere attachment. Following correction of measured spectra for interfacial reflections and edge losses, Kubelka–Munk theory was applied to estimate absorption and scattering coefficient, one-dimensional light intensity distribution, and light penetration depth. Kubelka–Munk absorption coefficients ranged from $\sim 7\ cm^{-1}$ at 330 nm to $\sim 1\ cm^{-1}$ at 850 nm. A localized absorption peak was noted at ~340 nm. Above 510 nm, weight-bearing cartilage demonstrated significantly higher absorption coefficients than nonweight-bearing tissue (paired t-test, $p<0.05$). Kubelka–Munk scattering coefficients ranged from $\sim 40\ cm^{-1}$ at 360 nm to $\sim 6\ cm^{-1}$ at 850 nm. No statistical differences in scattering coefficient were noted between weight-bearing and nonweight-bearing tissue. Penetration depths predicted by Kubelka–Munk theory ranged from 0.6 mm at 350 nm to over 3 mm at 850 nm. Stronger absorption in weight-bearing cartilage compared to nonweight-bearing tissue resulted in lower light penetration depths in weight-bearing cartilage at all wavelengths longer than 510 nm. [S1083-3668(98)01303-3]

Keywords absorption; scattering; Kubelka–Munk; penetration depth; intensity distribution; weight-bearing; nonweight-bearing.

1 INTRODUCTION

The use of lasers in orthopedic applications, while relatively new, is increasing. One of the most promising areas of orthopedic laser application is selective debridement of degenerative articular cartilage using the XeCl excimer laser emitting at 308 nm,[1–5] the 248 nm KrF excimer laser,[6] the Nd:YAG laser at 1,064 nm,[7,8] or the carbon dioxide laser at 10,600 nm.[7] Recently, the holmium:YAG laser emitting at 2,100 nm has also undergone extensive testing of its utility for cartilage debridement.[7,9] Among the advantages of using lasers for selective debridement of biomechanically compromised cartilage is the ability to spare the structurally intact tissue underlying the degenerative cartilage leaving a smooth articular surface through the process of thermally mediated collagen welding.[1,3,5]

In addition to the success achieved in laser-based cartilage debridement, laser irradiation has also been demonstrated to increase cartilage matrix metabolism *in vitro* and *in vivo* under certain laser delivery conditions,[7,8,10,11] although results have been mixed.[12,13] The biomodulatory mechanism of laser action is not currently known but studies are underway to elucidate the photobiologically active chromophores to optimally match the absorption spectrum of these chromophores to the appropriate laser wavelength.[7]

In most orthopedic laser applications, selectivity of laser absorption by the target tissue is an important factor in determining the success of the treatment. While some applications rely on selective ablation of articular cartilage, requiring strong absorption of the incident wavelength in the cartilage tissue, other applications target noncartilaginous tissues within the joint capsule. In the latter case, it is desirable to minimize laser-induced damage to articular cartilage. In order to optimize the choice of laser wavelength and energy delivery protocol to achieve the desired clinical outcome, it is necessary to understand how light of a given wavelength interacts with articular cartilage according to its spectral absorption characteristics. Minimization of damage to cartilage or to the adjacent, noncartilaginous tissue is also enhanced by knowledge of the laser energy distribution in the tissue as well as the depth of penetration into the target tissue and its underlying anatomical structures.

The purpose of this work was to quantitatively investigate the interaction of monochromatic light

Address all correspondence to Cynthia Roberts. Tel.: 614-292-1831; Fax: 614-292-7301; E-mail: Roberts.8@osu.edu

1083-3668/98/$10.00 © 1998 SPIE

with articular cartilage. To accomplish this, articular cartilage absorption and scattering coefficients were determined from 300 to 850 nm using spectrophotometer reflectance measurements and Kubelka–Munk theory. Differences in optical parameters between weight-bearing and nonweight-bearing articular cartilage were also investigated. Finally, the relative light intensity distribution and light penetration depth in articular cartilage were estimated using relationships derived from Kubelka–Munk theory. The 300–850 nm spectral range was examined because it encompasses several of the ultraviolet, visible, and near-infrared laser wavelengths currently used in clinical experimentation as well as some potentially useful laser wavelengths which have yet to be considered for clinical application.

2 METHODS

2.1 CARTILAGE HARVEST

Prior to processing, horses ($n=4$) used in this study were examined for indications of lameness or joint pathology. Immediately following euthanasia according to procedures approved by the Ohio State University Institutional Laboratory Animal Care and Use Committee, one stifle joint (the anatomical and functional equivalent to the human knee) was opened and the cartilage on the trochlear ridges and medial and lateral femoral condyles was determined to be grossly normal. Full thickness articular cartilage plugs were harvested using an 8 mm diameter biopsy punch and a scalpel. Tissue harvested from the medial and lateral condyles was considered to be weight-bearing while cartilage taken from the medial and lateral trochlear ridges was assigned to the nonweight-bearing group. Weight-bearing ($n=9$) and nonweight-bearing ($n=9$) cartilage specimens were stored separately in cold (4°C) saline solution.

2.2 PREPARATION FOR OPTICAL MEASUREMENTS

Within 24 hours of harvest, individual cartilage plugs were attached to the chuck of a vibrating microtome in preparation for sectioning. The nonarticulating side of the full thickness specimen was identified prior to the application of tissue adhesive (Vetbond, 3-M Company, Minneapolis, MN) to the cartilage plug. Following attachment of the cartilage plug to the microtome chuck, a 100 μm thick section was removed to create a level surface. The microtome blade was then lowered by 400 μm and another section sliced. In this fashion, all cartilage specimens were harvested within 500 μm of the articulating surface. Cartilage sections were stored in chilled saline solution awaiting further processing. Only one section per cartilage plug was used for spectrophotometric measurements.

To verify the thickness of the cartilage sections, each section was placed between two glass microscope slides of known thickness. The thickness of the slide-cartilage-slide assembly was measured with a micrometer by advancing the barrel of the micrometer onto the surface of the glass slides until slight resistance was felt. The combined thickness of the two microscope slides was subtracted from the total measured thickness to yield the thickness of the cartilage sample to a resolution of 0.001 inches (25.4 μm).

Since measured cartilage section thickness is a strong function of the pressure exerted by the micrometer during measurement, a preliminary study was accomplished to determine the precision of the microtome thickness measurements. Multiple micrometer measurements made on 38 cartilage sections of various thicknesses demonstrated that measurements were repeatable to within $\sim$32 μm. For spectrophotometric measurements, only cartilage sections measured to be 400 ± 50 μm were used.

2.3 SPECTROPHOTOMETER MEASUREMENTS

A dual beam diffuse reflectance spectrophotometer with integrating sphere attachment (Perkin-Elmer Corp., Lambda 6 Spectrophotometer, Norwalk, CT) was used to make reflectance measurements on individual articular cartilage specimens. A custom designed tissue mask was used throughout the experiment. The tissue mask consisted of a thin aluminum sheet, painted flat white, containing a 5 mm diameter hole aligned with the center of the incident beam. The mask was angled at approximately 8° to allow for collection of specularly reflected light in the integrating sphere.

Following background correction of the spectrophotometer, two scans were recorded and averaged with the tissue mask in place backed by a calibrated white porcelain tile. Two additional scans were recorded with the mask backed by a calibrated black porcelain tile. Individual 400 μm thick cartilage sections were then centered behind the hole in the mask and backed with the white and black porcelain tiles in turn. All reflectance measurements were recorded from 300 to 850 nm at 1 nm intervals. Measured reflectance was converted to absolute reflectance using software which accounted for the mask in the beam path and the known reflectance spectra of the two calibrated backing tiles. All reflectance measurements were converted to absolute reflectance by the use of a reflectance standard traceable to the National Institute of Standards and Technology.[14] Absolute reflectance spectra were pooled to generate weight-bearing and nonweight-bearing mean reflectance spectra.

2.4 KUBELKA–MUNK ANALYSIS

The Kubelka–Munk light propagation model[15] was used to calculate the Kubelka–Munk absorption coefficient (K) and scattering coefficient (S) for

weight-bearing and nonweight-bearing articular cartilage as a function of wavelength from spectrophotometer measurements of absolute reflectance.

The Kubelka–Munk model assumes that light incident on a slab of tissue backed by a reflective backing can be modeled by two fluxes, counterpropagating in the tissue slab. The optical flux, i, which propagates in the same direction as the incident flux, is decreased by absorption and scattering processes by an amount di as it passes through differential thickness dx. The fraction of i lost by absorption per unit path length is denoted K while the fraction lost due to scattering is called S. Flux i is also increased by back-scattering of the counterpropagating flux, j, into the same direction as i. Changes in flux j are determined in an analogous manner. Two differential equations describe the change in i and j during propagation through thickness dx:[15]

$$-\frac{di}{dx}=-(S+K)i+Sj, \tag{1}$$

$$\frac{dj}{dx}=-(S+K)j+Si \tag{2}$$

with the following boundary conditions:[16]

$$j=0 \text{ at } x=0 \text{ and } I=I_{\text{inc}} \text{ at } x=X, \tag{3}$$

where $x=0$ refers to the back, nonincident surface of the tissue slab, X is the total thickness of the tissue slab, and I_{inc} is the intensity of the incident light. The hyperbolic solution to this set of differential equations is:[15]

$$i(x)=I_{\text{inc}}\left[\frac{a\ \sinh(bSx)+b\ \cosh(bSx)}{a\ \sinh(bSX)+b\ \cosh(bSX)}\right], \tag{4}$$

$$j(x)=I_{\text{inc}}\left[\frac{\sinh(bSx)}{a\ \sinh(bSX)+b\ \cosh(bSX)}\right], \tag{5}$$

where[15]

$$a=1+\frac{K}{S}, \tag{6}$$

$$b=\sqrt{a^2-1}. \tag{7}$$

Further manipulation yields:[15]

$$R_{K-M}=\frac{1-R_g[a-b\ \text{ctgh}(bSX)]}{a-R_g+b\ \text{ctgh}(bSX)}, \tag{8}$$

where R_{K-M} is the reflectance of the tissue on the backing, R_g is the reflectance of the backing, and ctgh is the hyperbolic cotangent function. Since R_{K-M} can be derived from measurements of total reflectance, and R_g, and X are directly measurable, Eq. (8) contains two unknowns: K and S. The use of two backings with different reflectances permitted the development of two equations in two unknowns. A solution at each wavelength provided the desired optical coefficients, K and S.

2.5 ASSUMPTIONS IN KUBELKA–MUNK THEORY

Several assumptions accompany use of the basic Kubelka–Munk theory described above,[15,17] each of which was addressed in this work. The first assumption is that while K and S are known to be a strong function of wavelength, they are assumed to be uniform throughout the tissue slab. Since only the first 500 μm thick layer of cartilage was used to make the reflectance measurements, K and S were not expected to vary significantly in that layer. Based on the layered configuration of cartilage, however, it is possible that K and S would vary as a function of depth in a full thickness cartilage sample. In this work, no attempt was made to measure K and S as a function of depth in the cartilage samples.

The second assumption is that all light fluxes are diffuse. According to van Gemert,[18] if the mean free scattering path length of a sample is much smaller than its thickness, the incident flux is quickly scattered and becomes diffuse in a very short distance within the sample. In cartilage this assumption is appropriate in the ultraviolet and visible region due to relatively high scattering. In the infrared region, the mean free scattering path length increases as scattering decreases, and the incident flux may not become as quickly diffuse. The mean free path length can be estimated for cartilage in this region by assuming an anisotropy of 0.8, a value consistent with the range of most tissues.[19] This yields a mean free scattering path length of approximately half the sample thickness in the infrared. Therefore, the infrared light may not become immediately diffuse and the Kubelka–Munk model may be less accurate in this region.

Modification to the basic Kubelka-Munk formulation to add a third, collimated flux in the direction of the incident irradiation has been attempted.[20] Although this model may improve values in the infrared region, the 3-Flux theory, when used to determine the optical properties of maxillofacial materials, was found to provide a relatively small improvement in accuracy over the basic Kubelka–Munk two flux model at the cost of significantly greater mathematical complexity.[20]

2.6 CORRECTION FOR INTERFACIAL REFLECTIONS

Basic Kubelka–Munk theory does not account for reflections at boundaries at which index of refraction mismatches exist. In this experimental setup, reflections due to index of refraction mismatches occur at the air-tissue surface interface, internally at the tissue-air interface, and at the tissue-backing interface.

The index of refraction of articular cartilage was estimated based on a relationship developed by Wilson and Jacques[21] which approximates the index of refraction of a material based on its water content:

$$n \approx (1.53 - 0.2W), \tag{9}$$

where W is the percentage water content of the tissue. Assuming a value of 75% for W,[22] the index of refraction of articular cartilage was found to be 1.38. This value is well within the range of refractive index normally associated with mammalian tissue.[23] The index of refraction of the porcelain tile backings was 1.5. There was no attempt made to account for changes in index of refraction with wavelength.[23]

The relationship which specifies how the measured reflectance, R, should be corrected for the two interfacial reflections which occur at the front surface of the sample is:[24]

$$R = r_0 + \frac{(1-r_0)(1-r_i)R_{K-M}}{1-r_i R_{K-M}}, \tag{10}$$

where r_0 is the fraction of light reflected at the air-tissue interface as light enters the sample (the external reflection), r_i is the fraction of diffuse light internally reflected as light leaves the sample and re-enters the air, and R_{K-M} is the tissue reflectance required to determine the Kubelka–Munk optical coefficients. Equation (10) is rearranged to yield R_{K-M} as a function of measured reflectance, R, and the interfacial reflection corrections:[25]

$$R_{K-M} = \frac{R - r_0}{1 + r_i R - r_0 - r_i}. \tag{11}$$

The reflection of near-normal collimated light occurring at the air-tissue interface, r_0, was determined by the Fresnel equation,[21] where n is the index of refraction of the cartilage sample:

$$r_0 = \left[\frac{(n-1)}{(n+1)}\right]^2. \tag{12}$$

For an index of refraction of cartilage of 1.38, Eq. (12) yields a value of 0.0255. The fraction of diffuse light internally reflected as it leaves the sample at the front surface and re-enters the air, r_i, was modeled by the equation:[14]

$$r_i = 1 - \frac{1-r_d}{n^2}, \tag{13}$$

where r_d is the reflection factor for diffuse incident light and is given by:[20]

$$r_d = \frac{1}{2} + \frac{(n-1)(3n+1)}{6(n+1)^2} + \frac{n^2(n^2-1)^2}{(n^2+1)^3}\ln\left(\frac{n-1}{n+1}\right) - \frac{2n^3(n^2+2n-1)}{(n^2+1)(n^4-1)} + \frac{8n^4(n^4+1)}{(n^2+1)(n^4-1)^2}\ln(n). \tag{14}$$

For an index of refraction of cartilage of 1.38, the value calculated for r_i was 0.514. The refraction occurring at the tissue-backing interface was neglected since the index of refraction mismatch was small at this boundary.

2.7 CORRECTION FOR EDGE LOSS

The last assumption in Kubelka–Munk theory is that the amount of light lost from the edges of the sample during reflectance measurement is negligible. The amount of edge loss which occurred during reflectance measurements of articular cartilage was approximated by using a procedure which compared the reflectance from samples contained in conventional holders, which allowed edge loss, to samples contained in custom holders, which used polished aluminum edges to redirect light escaping at the edges back into the sample.[24] The difference in reflectance in these two cases was modeled by regression analysis using the term b^*S as the parameter of interest. Both b and S have been defined previously. Individual regression equations were fit for white and black backings over a range of bS values.[24]

To correct the data in this work for edge losses, an iterative procedure was implemented in which R_{K-M}, after correcting for interfacial reflections, was used to find K and S at each wavelength assuming no edge losses were present. Once K and S were known, bS was determined from:[24]

$$bS = \sqrt{(2KS + K^2)}. \tag{15}$$

This value of bS was used in the appropriate regression equation to approximate the amount of edge loss expected at the given wavelength. The amount of edge loss predicted by the regression equation was then added back to the original value of R_{K-M} and new values of K and S calculated at that wavelength. Iteration was ceased when the correction factor applied to R_{K-M} was less than 1% based on the most recently calculated values of K and S. Average estimated edge loss over all wavelengths was approximately 4%.

2.8 CALCULATION OF DERIVED QUANTITIES

Addition of the counter-propagating optical fluxes, $i(x)$ and $j(x)$, at a given depth in the tissue yielded an estimate of the total on-axis light intensity at a given wavelength:[16]

$$\frac{I(x)}{I_{\text{inc}}} = \frac{i(x)+j(x)}{I_{\text{inc}}} = \left[\frac{(a+1)\sinh(bSx)+b\cosh(bSx)}{a\sinh(bSX)+b\cosh(bSX)}\right]. \quad (16)$$

The relative intensity, $I(x)/I_{\text{inc}}$, is the ratio of the central beam axis intensity at depth x to the intensity of the incident light.[15] Calculations of relative intensity were made at 10 nm intervals from 300 to 850 nm.

Each relative intensity distribution developed from Kubelka–Munk theory was fit to an exponential function of the form:

$$\frac{I(d)}{I_{\text{inc}}} = \frac{I(d)}{I(d=0)} = e^{-\gamma d}. \quad (17)$$

In this equation, the total attenuation coefficient, γ, denotes the decrease of the incident intensity per unit path length via combined tissue absorption and scattering mechanisms. The depth at which the total light intensity was attenuated to $1/e$ (37%) and $1/e^2$ (13.5%) of the incident intensity was determined at 50 nm intervals from 300 to 850 nm.

Finally, using van Gemert and Star's conversions for anisotropic scattering,[26] values of K and S derived from Kubelka–Munk theory were converted to optical transport properties for ease of comparison with optical properties in the scientific literature. The relevant equations were:[26]

$$\mu_a = \eta K, \quad (18)$$

$$\mu_s' = \chi S, \quad (19)$$

$$\frac{K}{S} = \frac{\chi}{\eta}\left(\frac{1-W_0}{W_0}\right), \quad (20)$$

where

$$\eta = \frac{(\phi-1)(1-W_0)}{\xi(\phi+1)},$$

$$\chi = \frac{-W_0}{2\xi}(\phi-\phi^{-1}),$$

$$W_0 = \frac{2\xi}{\ln\{(1+\xi)/(1-\xi)\}},$$

and

$$\phi = \frac{\xi+\ln(1-\xi)}{\xi-\ln(1+\xi)}.$$

Note that μ_s' is the reduced scattering coefficient, equal to $\mu_s(1-g)$, with g corresponding to the scattering anisotropy factor.

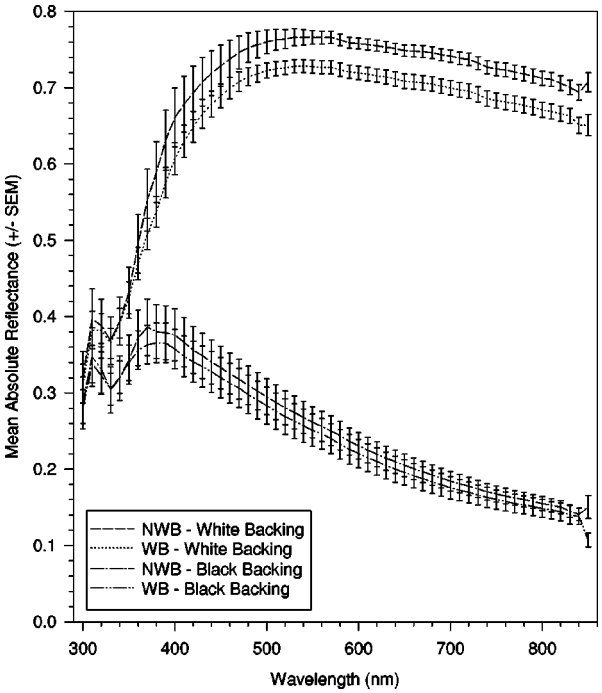

Fig. 1 Average reflectance profiles for nonweight-bearing ($n=9$) and weight-bearing ($n=9$) articular cartilage sections backed by white and black porcelain backing tiles from 300–850 nm.

2.9 STATISTICAL ANALYSIS

Spectrophotometer measurements of reflectance were accomplished at 1 nm wavelength intervals over the range 300 to 850 nm. All figures in this work were generated using data at 10 nm or 50 nm intervals as indicated. Paired t-tests at a significance level of $\alpha=0.05$ were used to test for differences between weight-bearing ($n=9$) and nonweight-bearing ($n=9$) absorption and scattering coefficients at 10 nm wavelength intervals.

3 RESULTS

3.1 ABSORPTION AND SCATTERING COEFFICIENTS

Kubelka–Munk absorption and scattering coefficients (Figure 2) derived from application of Kubelka–Munk theory to articular cartilage reflectance spectra (Figure 1) demonstrated several trends. Absorption was maximal at ultraviolet wavelengths but remained relatively constant at wavelengths longer than ~500 nm. A local absorption maximum located at ~340 nm (Figure 2) was also evident. At wavelengths longer than 510 nm, weight-bearing samples demonstrated statistically greater absorption than nonweight-bearing samples. Scattering was also maximal at shorter wavelengths with a rapid decrease in scattering noted at longer wavelengths. Between 330 nm and 350 nm, there was a localized decrease in scattering corresponding to the increased absorption in this range. At all wavelengths tested, scattering domi-

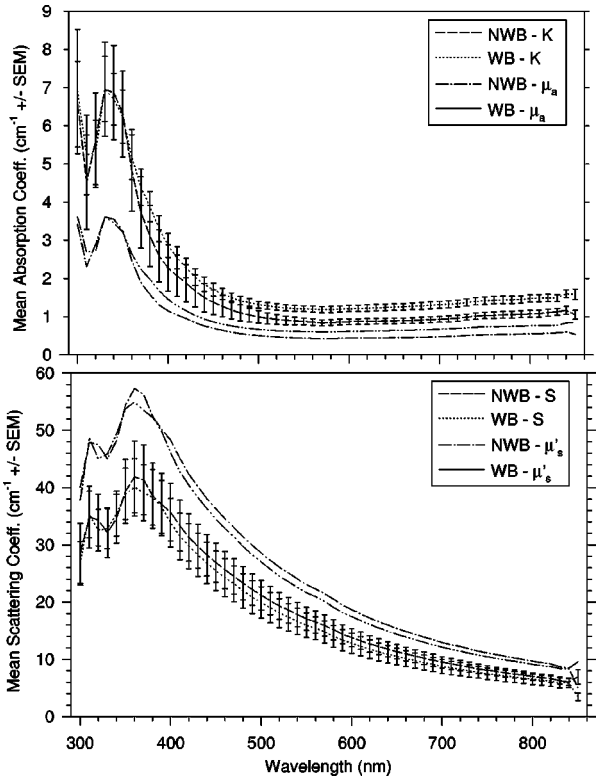

Fig. 2 Kubelka–Munk absorption (K) and scattering (S) coefficients calculated from absolute reflectance measurements from 300–850 nm. At wavelengths longer than 510 nm, weight-bearing cartilage demonstrated significantly stronger absorption than nonweight-bearing tissue ($p<0.05$). Scattering coefficient was not significantly different at any wavelength. Optical transport coefficients (μ_a and μ_s') calculated from K and S are also shown.

nated absorption. There was no difference noted at any wavelength between weight-bearing and nonweight-bearing tissue in terms of Kubelka–Munk scattering coefficient. Trends noted in optical transport coefficients shown in Figure 2 match those demonstrated by Kubelka–Munk coefficients.

3.2 RELATIVE INTENSITY DISTRIBUTION

Based on the preferential absorption and dominant scattering demonstrated in articular cartilage at shorter wavelengths, incident ultraviolet light (<400 nm) was rapidly attenuated in this tissue (Figure 3). In wavelength regions in which absorption and scattering were both minimized, attenuation of incident light was much less rapid. At 1 mm below the surface of the cartilage on which the light was incident, over 80% of the incident intensity of 850 nm wavelength light was present while less than 20% of 300 nm light intensity remained at the same depth (Figure 3). Values of the intensity profile which exceeded 100% indicate the presence of backscattered light predicted by the Kubelka–Munk model.

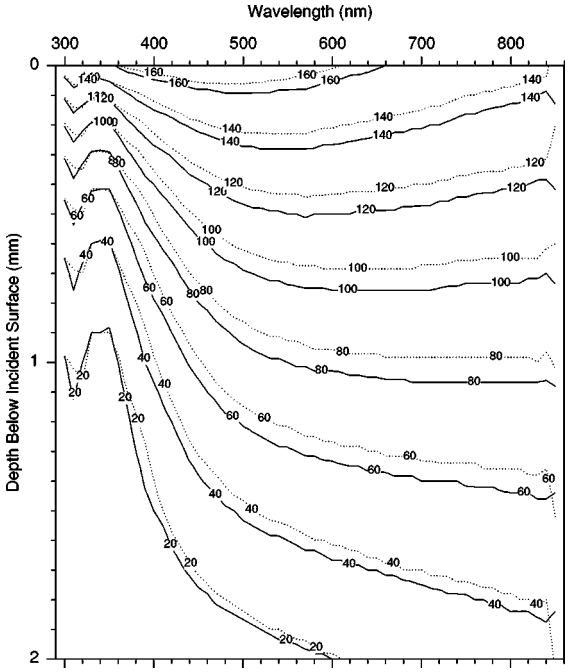

Fig. 3 Contour plot of the relative light intensity distributions for articular cartilage samples calculated from Kubelka–Munk theory from 300 to 850 nm. Contours are shown for nonweight-bearing (solid lines) and weight-bearing (dotted lines) tissue. Contours labels represent the percentage of incident intensity which remains at the given depth in the cartilage sample.

3.3 PENETRATION DEPTH

The depth at which the incident light intensity was attenuated to 37% of its initial value ($1/e$ depth) varied from approximately 0.6 mm at 350 nm wavelength to approximately 3.4 mm at 850 nm in this tissue (Figure 4). The depth at which the incident light intensity was attenuated to 13.5% of its initial value ($1/e^2$ depth) ranged from 1.3 mm at 350 nm to 6.8 mm at 850 nm wavelength. Deep penetration depths noted in articular cartilage, especially at longer wavelengths, reflected the weak absorption and reduced scattering at these wavelengths. The region of preferential absorption noted at ~340 nm was also apparent in the penetration depth curves as a localized reduction in penetration depth. In addition, stronger absorption of light in weight-bearing cartilage was evident as a shallower penetration depth relative to nonweight-bearing tissue at all wavelengths above approximately 350 nm. At longer wavelengths, the difference between the 13.5% penetration depth in the nonweight-bearing and weight-bearing, was approximately 1 mm.

4 DISCUSSION

Although optical properties of many mammalian tissues have been reported, articular cartilage has been generally ignored, even in light of the increasing use of lasers in joint surgery. Raunest and Schwarzmaier[27] measured the optical density of healthy human hyaline cartilage from 250 to 770

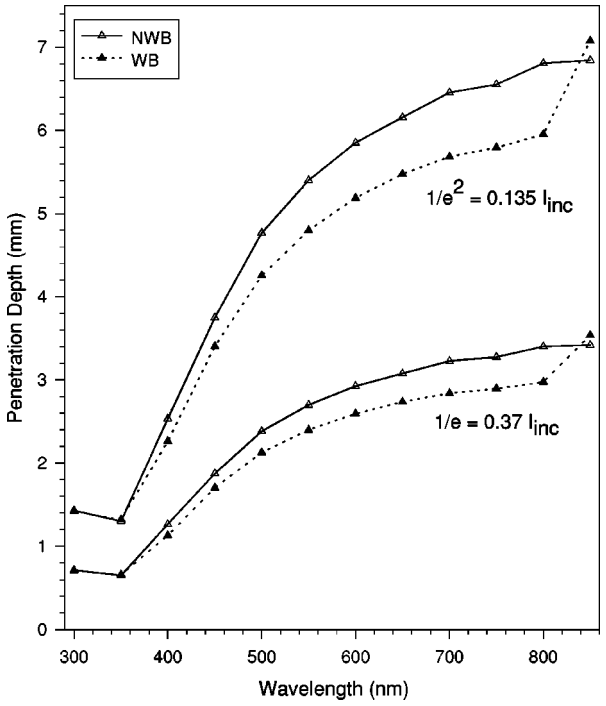

Fig. 4 Light penetration depth for weight-bearing and nonweight-bearing articular cartilage assuming exponential light attenuation.

nm, reporting a preferential absorption peak at 280 nm rather than in the 330–350 nm range found in this study. These authors did not include calculation of absorption or scattering coefficient, light intensity profiles, penetration depth, or differences between weight-bearing and nonweight-bearing cartilage.

Vangsness et al.[28] spectrophotometrically measured the absorption spectra of fibrocartilaginous human menisci from 300 to 2500 nm and found steadily decreasing absorption in the wavelength range from 300 to 1000 nm, partially confirming the results found in this work. These authors also noted a localized absorption peak at approximately 300 nm attributable to the presence of collagen proteins.[28] This study did not include, however, data related to scattering behavior, determination of optical coefficients, or penetration depth as a function of wavelength.

The local articular cartilage absorption peak at ~340 nm represents a potentially useful finding for enhancing the selectivity of laser application to this tissue. For applications requiring direct targeting of articular cartilage and preferred absorption of incident energy, use of a nitrogen laser (337 nm) or a frequency tripled Nd:YAG laser (335 nm) may prove advantageous, in that absorption of laser energy will be maximized at these wavelengths. Likewise, if the application requires delivery of laser energy to tissues in close proximity to articular cartilage, the 337 nm wavelength should be avoided when choosing the laser system in order to minimize absorption by the nontargeted cartilage. Prior to selection of the laser system on this basis, however, the spectra of adjacent tissues such as the menisci and the synovium must also be considered. Furthermore, optical properties of articular cartilage are altered during laser irradiation, as demonstrated by Raunest and Schwarzmaier,[27] complicating the choice of laser wavelength.

Another notable finding was that the penetration depths calculated for this tissue were fairly large for visible and infrared wavelengths due to the weak absorption demonstrated by articular cartilage. Since the cartilage covering the surface of the femoral condyles in humans is generally 2–3 mm thick,[29] large penetration depths may result in a significant fraction of the laser energy incident on the articulating surface of the cartilage, penetrating into the underlying subchondral bone. Use of a laser system emitting in the ultraviolet can take advantage of the relatively strong absorption of articular cartilage in this wavelength region to preclude involvement of the underlying anatomy and promote the selective ablation of articular cartilage.

In summary, articular cartilage was shown to possess very weak absorption properties in the 300–850 nm wavelength range with scattering dominating absorption at all wavelengths. The absorption characteristics of weight-bearing and nonweight-bearing articular cartilage show similar trends with wavelength although weight-bearing cartilage absorbs more strongly at wavelengths longer than 510 nm. Due to the weak absorption of articular cartilage and the subsequently large penetration depths, laser irradiation of articular cartilage at longer wavelengths almost certainly involves deposition of significant laser energy into the subchondral bone.

Acknowledgments

This work was supported by the Whitaker Foundation. The authors thank Dr. Emily Simmons, Dr. Susan Volman, and Ms. Robin Nakkula for their assistance in tissue collection and preparation.

REFERENCES

1. K. A. Athanasiou, R. Fischer, G. G. Niederauer, and W. Puhl, ''Effects of excimer laser on healing of articular cartilage in rabbits,'' *J. Orthop. Res.* **13**, 483–494 (1995).
2. R. Fischer, R. Hibst, D. Schroder, W. Puhl, and R. Steiner, ''Thermal side effects of fiber-guided XeCl excimer laser drilling of cartilage,'' *Lasers Surg. Med.* **14**, 278–286 (1994).
3. R. Fischer, R. Krebs, and H. P. Scharf, ''Cell vitality in cartilage tissue culture following excimer laser radiation: an in vitro examination,'' *Lasers Surg. Med.* **13**, 629–637 (1993).
4. N. D. Glossop, R. W. Jackson, H. J. Koart, S. C. Reed, and J. A. Randle, ''The excimer laser in orthopaedics,'' *Clin. Orthop. Rel. Res.* **310**, 72–81 (1995).
5. J. Raunest and J. Lohnert, ''Arthroscopic cartilage debridement by excimer laser in chondromalacia of the knee joint,'' *Arch. Orthop. Trauma Surg.* **109**, 155–159 (1990).
6. Y. Freedland, ''Use of excimer laser in fibrocartilaginous excision from adjacent bony stroma: a preliminary investigation,'' *J. Foot Surg.* **27**(4), 303–305 (1988).
7. C. T. Vangsness and B. Haderi, ''A literature review of la-

sers and articular cartilage,'' *Lasers Orthop. Surg.* **16**, 593–598 (1993).
8. D. V. Miller, S. J. O'Brien, S. S. Arnoczky, A. Kelly, S. V. Fealy, and R. F. Warren, ''The use of contact Nd:YAG laser in arthroscopic surgery: effects on articular cartilage and meniscal tissue,'' *Arthroscopy* **5**(4), 245–253 (1989).
9. M. A. Collier, L. M. Haugland, J. Bellamy, L. L. Johnson, M. D. Rohrer, R. C. Walls, and K. E. Bartels, ''Effects of holmium:YAG laser on equine articular cartilage and subchondral bone adjacent to traumatic lesions: a histopathological assessment,'' *Arthroscopy* **9**(5), 536–545 (1993).
10. J. H. Herman and R. C. Khosla, ''In vitro effects of Nd:YAG laser radiation on cartilage metabolism,'' *J. Rheumatol.* **15**, 1818–1826 (1988).
11. J. M. Spivak, D. A. Grande, A. Ben-Yishay, D. S. Menche, and M. I. Pitman, ''The effect of low-level Nd:YAG laser energy on adult articular cartilage in vitro,'' *Arthroscopy* **8**, 36–43 (1992).
12. E. M. Hardie, C. S. Carlson, and D. C. Richardson, ''Effect of Nd:YAG laser energy on articular cartilage healing in the dog,'' *Lasers Surg. Med.* **9**, 595–601 (1989).
13. B. Rogvi-Hansen, N. Ellitsgaard, M. Funch, M. Dall-Jensen, and J. Prieske, ''Low level laser treatment of chondromalacia patellae,'' *Int. Orthop.* **15**, 359–361 (1991).
14. W. M. Johnston, W. J. O'Brien, and T. Y. Tien, ''The determination of optical absorption and scattering in translucent porcelain,'' *Color Res. Appl.* **11**(2), 125–130 (1986).
15. P. Kubelka, ''New contributions to the optics of intensely light-scattering materials: Part I,'' *J. Opt. Soc. Am.* **38**(5), 448–457 (1948).
16. M. J. C. van Gemert and J. P. H. Henning, ''A model approach to laser coagulation of dermal vascular lesions,'' *Arch. Dermatol Res.* **270**, 429–439 (1981).
17. D. B. Judd and G. Wyszecki, Eds., ''Physics and psychophysics of colorant layers,'' Chap. 3 in *Color in Business, Science, and Industry,* pp. 398–462, Wiley, New York (1975).
18. M. J. C. van Gemert, A. J. Welch, W. M. Star, M. Motabedi, and W. Cheong, ''Tissue optics for a slab geometry in the diffusion approximation,'' *Lasers Med. Sci.* **2**, 295–305 (1987).
19. W. F. Cheong, S. A. Prahl, and A. J. Welch, ''A review of the optical properties of biological tissues,'' *IEEE J. Quantum Electron.* **26**(12), 2166–2185 (1990).
20. N. S. Hesse, ''Concentration additivity of optical coefficients for pigment mixtures in maxillofacial elastomer,'' Masters Thesis, The Ohio State University (1993).
21. B. C. Wilson and S. L. Jacques, ''Optical reflectance and transmittance of tissues: principles and applications,'' *IEEE J. Quantum Electron.* **26**(12), 2186–2199 (1990).
22. R. J. Todhunter and G. Lust, ''Synovial joint anatomy, biology, and pathbiology,'' Chap. 79 in *Equine Surgery*, J. A. Auer, Ed., pp. 844–866, WB Saunders Co., Philadelphia, PA (1992).
23. F. P. Bolin, L. E. Preuss, R. C. Taylor, and R. J. Ference, ''Refractive index of some mammalian tissues using a fiber optic cladding method,'' *Appl. Opt.* **28**(12), 2297–2303 (1989).
24. W. M. Johnston, N. S. Hesse, B. K. Davis, and R. R. Seghi, ''Analysis of edge-losses in reflectance measurements of pigmented maxillofacial elastomer,'' *J. Dental Res.* **75**(2), 752–760 (1996).
25. G. D. Woolsey, W. M. Johnston, and W. J. O'Brien, ''Masking power of dental opaque porcelains,'' *J. Dental Res.* **63**(6), 936–939 (1984).
26. M. J. C. van Gemert and W. M. Star, ''Relations between the Kubelka-Munk and the transport equation models for anisotropic scattering,'' *Laser Life Sci.* **1**(4), 287–298 (1987).
27. J. Raunest and H. J. Schwarzmaier, ''Optical properties of human articular tissue as implication for a selective laser application in arthroscopic surgery,'' *Lasers Surg. Med.* **16**, 253–261 (1995).
28. C. T. Vangsness, J. Huang, and C. F. Smith, ''A spectrophotometer analysis of light absorption in the human meniscus,'' *Clin. Orthop. Rel. Res.* **310**, 27–29 (1995).
29. E. B. Hunziker, ''Articular cartilage structure in humans and experimental animals,'' Chap. 13 in *Articular Cartilage and Osteoarthritis*, K. Kuettner, Ed., pp. 183–199, Raven Press, Ltd., New York (1992).